

Defect-Induced Magnetic Skyrmion in Two-Dimensional Chromium Tri-Iodide Monolayer

Ryan A. Beck, Lixin Lu, and Xiaosong Li*

Department of Chemistry, University of Washington, Seattle, WA, 98195

Peter V. Sushko

*Physical Sciences Division, Physical & Computational Sciences Directorate,
Pacific Northwest National Laboratory, Richland, WA, 99352*

Xiaodong Xu

Department of Physics, University of Washington, Seattle, WA, 98195

(Dated: March 5, 2021)

Chromium iodide monolayers, which have different magnetic properties in comparison to the bulk chromium iodide, have been shown to form skyrmionic states in applied electromagnetic fields or in Janus-layer devices. In this work, we demonstrate that spin-canted solutions can be induced into monolayer chromium iodide by select substitution of iodide atoms with isovalent impurities. Several concentrations and spatial configurations of halide substitutional defects are selected to probe the coupling between the local defect-induced geometric distortions and orientation of chromium magnetic moments. This work provides atomic-level insight into how atomically precise strain-engineering can be used to create and control complex magnetic patterns in chromium iodide layers and lays out the foundation for investigating the field- and geometric-dependent magnetic properties in similar two-dimensional materials.

I. INTRODUCTION

Magnetic skyrmions are local whirls of the spins that both have a fixed chirality and do a full spin rotation.¹ Isolated skyrmions can be treated as single particles and used in applications, such as system memory, radio frequency generators and filters, as well as spintronic devices.^{1,2} Typically, skyrmion formation in materials involves breaking their inversion symmetry which enables an asymmetric exchange interaction, the Dzyaloshinskii-Moriya interaction (DMI), through spin-orbit coupling. The DMI interaction takes the form:³

$$H_{DMI} = (S_1 \times S_2) \cdot \mathbf{d}_{12} \quad (1)$$

where S_1 and S_2 are spins of two neighboring magnetic atoms and \mathbf{d}_{12} is the corresponding Dzyaloshinskii-Moriya vector. If the exchange interaction between S_1 and S_2 is mediated by an anion, \mathbf{d}_{12} can be written as $\mathbf{d}_{12} = \mathbf{r}_1 \times \mathbf{r}_2$, where \mathbf{r}_1 and \mathbf{r}_2 link the anion with the two magnetic ions.⁴ In CrX_3 , this term is missing as the contributions associated with anionic pathways linking two neighboring Cr centers cancel out due to inversion symmetry. Commonly, skyrmion formation is induced by the application of an external electromagnetic field which, in the case of CrX_3 , breaks the inversion symmetry of the system allowing the spins of the Cr centers to rotate. It has also been reported that Janus CrX_3 monolayers stabilize skyrmions.^{1,2,5-7} Ideally, for practical use, materials would be able to realize skyrmions at high temperatures (those approaching room temperature) at zero, or very small, field strengths.¹

Chromium trihalides and, more broadly, MX_3 (where M is a transition metal) compounds are actively investi-

gated for their unusual properties. They have a low synthesis and processing cost and can be easily exfoliated to obtain few-layer materials. In chromium trihalide (CrX_3 , $X=\text{Cl, Br, I}$) structures, the Cr^{3+} ions are arranged into honeycomb lattices surrounded by six halogen anions giving rise to local octahedral symmetry. The halogen atoms are each bound to two neighboring Cr centers. At high temperature the layers stack with a monoclinic (space group $C2/m$) geometry. At low temperature the layers stack with a rhombohedral (space group $R\bar{3}$) geometry. The temperature at which this transformation occurs is dependent on the halogen ($\text{Cl}=240$ K, $\text{Br}=420$ K, and $\text{I}=210$ K), and each bulk structure is known to have ferromagnetic moments between each Cr ion below their T_c ($\text{Cl}=17$ K, $\text{Br}=37$ K, and $\text{I}=68$ K).^{12,19} Examples of the monolayer, hexagonal lattice and the bulk stacking can be seen in the insets to Fig. 1.

CrI_3 bulk has been shown to exhibit the highest reported magnetic ordering temperature and anisotropy among the chromium trihalides.^{8,12-15} It has been shown that in the low-layer limit (number of layers $<\sim 10$), MX_3 exhibit magnetic properties which appear to differ from their bulk properties.⁸⁻¹¹ Recently, mono- and bi-layers of chromium trihalide materials have been investigated for potential use in skyrmionic devices.^{1,2,6,16}

Monolayer CrI_3 is known to have long-range ferromagnetic character, in disagreement with the Mermin-Wagner theorem,^{2,17} which is enabled through the magnetic anisotropy.^{2,18} This magnetic anisotropy in CrI_3 arises from the spin-orbit coupling in iodine atoms, and favors a magnetic easy axis perpendicular to the atomic plane.^{4,18,19} Magnetic interactions between the chromium ions in a CrI_3 layer arise from a superexchange mechanism between the Cr $3d$ orbitals and the

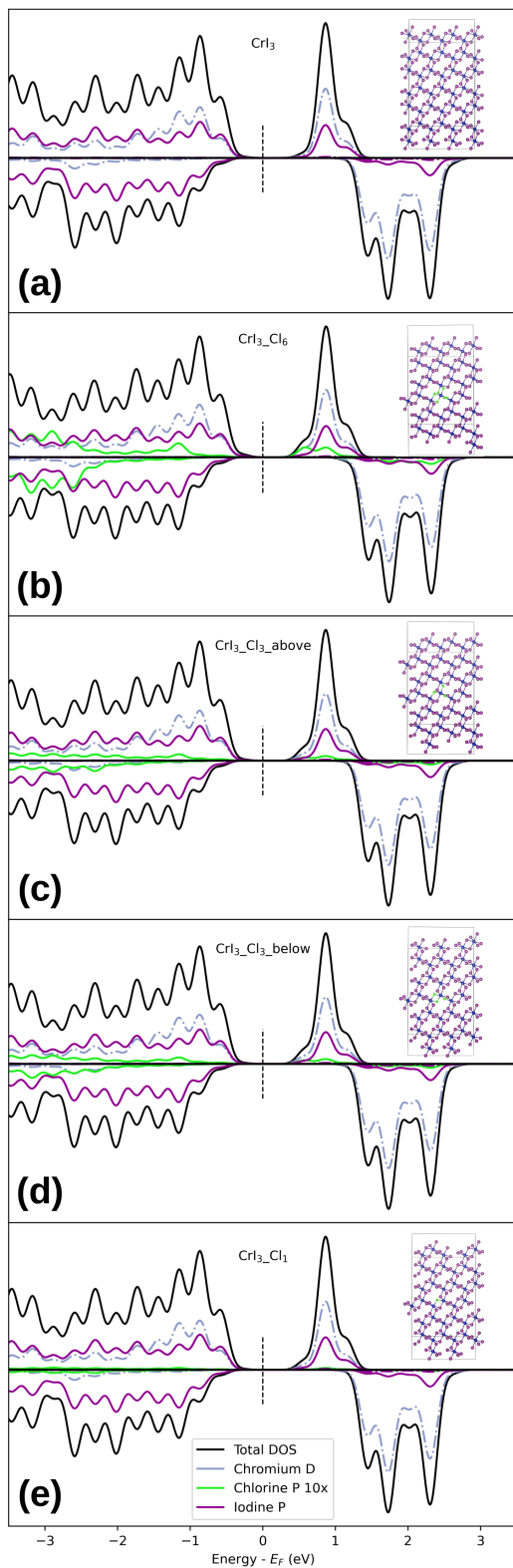


FIG. 1. The spin-resolved projected density of states for the monolayer CrI_3 systems (shown as insets to each plot). The total DOS can be seen in each plot as the black line, the projected orbital contributions for the Cr-d (blue), I-p (purple), and Cl-p (green) atoms are plotted as well. The pure CrI_3 monolayer system is shown at the top (a), with the halogen-replaced structures shown beneath: $\text{CrI}_3\text{-Cl}_6$ (b), $\text{CrI}_3\text{-Cl}_3\text{-above}$ (c), $\text{CrI}_3\text{-Cl}_3\text{-below}$ (d), and $\text{CrI}_3\text{-Cl}_1$ (e).

I 5p orbitals.^{4,11,18,20} Geometric distortions in the CrI_3 layers can break the inversion symmetry, and thus induce finite Dzyaloshinskii-Moriya interaction, ultimately leading to the appearance of skyrmionic ground states. In the case of an applied electric field oriented perpendicular to the CrI_3 plane, the Cr^{3+} and I^- ions displace in the opposite directions in and out of the plane. These displacements change distances between the chromium and iodine atomic planes by as much as $\sim 3.6\%$ for the field magnitude of ~ 0.2 V/nm, resulting in significant DMI effects.

In this work we investigate the formation of skyrmionic states via breaking the inversion symmetry of the CrI_3 monolayer by substituting iodine atoms with chloride atoms (Cl_I). Unlike external electric fields, these defects produce localized atomic-scale distortions, which holds the promise of creating fine-tuned distortion patterns and, accordingly, may enable the formation of complex magnetic structures.

II. METHODOLOGY

Monolayer CrI_3 was represented using the isolated periodic slab model. The initial positions of atoms correspond to the bulk CrI_3 lattice as determined through single crystal X-ray diffraction at 90 K.¹² To find the optimal structure of the monolayer and its electronic properties, we performed ab initio simulations based on the density functional theory (DFT) as implemented in the Vienna *ab initio* simulation program (VASP).^{21,22} The projector augmented wave method and Perdew-Burk-Ernzerhof exchange correlation functional were used.^{23,24} The calculations were performed in the spin-polarized mode. A plain-wave basis set was used with an energy cutoff of 600 eV, and the DFT-D3(0)²⁵ method was used for dispersion correction. All internal coordinates were fully relaxed. It has been noted that the Hubbard U correction applied within the DFT+U method does not significantly impact the results of the calculations, and as such is not used herein.^{4,18}

To find the properties of pristine CrI_3 , we used a supercell containing two chromium and six iodine atoms. A 3.5 nm vacuum gap in the off-plane direction (z) was used to avoid the monolayer interactions with its periodic images. The Brillouin zone was sampled with a Monkhorst-Pack k -point mesh of $6 \times 6 \times 2$. The optimal lattice constant (a_0) was found to be 6.929 Å, which is in a close agreement with the experimentally observed value of 6.866 Å.¹²

The calculated Heisenberg isotropic symmetric exchange coefficient ($J = -2.99$ meV) and the magnetic anisotropy energy (MAE) (0.58 meV/Cr) are comparable with those previously reported for the CrI_3 systems (less than 10 layers): $J = -2.2$ meV and MAE = 0.65 meV/Cr.^{2,4?}

In order to examine the magnetic effects of Cl substitution, we used a CrI_3 supercell of $1.8 \text{ nm} \times 3.1 \text{ nm}$

$\times 2.0$ nm. Several iodine atoms near a chromium center were replaced with Cl atoms, and the internal coordinates were optimized for each case. The cutoff for energy minimization with respect to the atomic coordinates was set to 10^{-5} eV. With the optimized structure, a noncollinear (NC) spin calculation was run with the self-consistent-field (SCF) convergence cutoff set to 10^{-6} eV. The noncollinear wavefunction was used as a guess for the calculations incorporating spin-orbit coupling effects (NC-SOC) with SCF convergence set to 10^{-9} eV in order to capture the energy cost of spin rotations which typically are on the order of $10^{-6} \sim 10^{-4}$ eV in magnitude.²

III. RESULTS AND DISCUSSION

A. Geometric Distortion

In an attempt to introduce unique magnetic properties, chlorine atoms have been introduced into the CrI_3 monolayer in various configurations. Chlorine was specifically chosen as it has been previously shown that bulk CrCl_3 exhibits an in-plane ferromagnetism,¹² which was thought could be taken advantage of to promote skyrmion formation without drastically altering the properties of the CrI_3 layer. Also, of the CrX_3 systems commonly examined, Cl has the smallest atomic radius, and as such is thought to give rise to the largest geometric distortions. Four $\text{CrI}_3\text{-Cl}_x$ structures were examined, and can be viewed in the insets for Fig. 1. The four geometries considered have six iodine centers replaced around a chromium center ($\text{CrI}_3\text{-Cl}_6$), three Cl replacing the iodine above the chromium atomic plane ($\text{CrI}_3\text{-Cl}_3\text{-above}$), three Cl replacing the iodine both above and below the chromium atomic plane ($\text{CrI}_3\text{-Cl}_3\text{-below}$), and one Cl replacing a single iodine atom ($\text{CrI}_3\text{-Cl}_1$).

As can be seen in Fig. 2, replacing I atoms with Cl atoms results in a contraction of the Cr-Cl bonds (in comparison to the Cr-I bonds) as is expected given that Cl is both smaller and more electronegative than I. In the case where six I atoms are replaced, the geometric distortions extend through the monolayer for ~ 1.7 nm, similar to the extent of skyrmion formation which has been observed when CrI layers are exposed to a field.² It should be noted that this size may be artificially constrained due to the size of the cluster used, as was also noted for the skyrmion formation by Liu *et al.* (Ref. 2). This distortion is shown in Fig. 2a as the circle of diameter $d_a = 1.7$ nm. For systems where less Cl has been doped into the cell (in Fig. 2b-d) the extent of the distortion caused is lessened. $\text{CrI}_3\text{-Cl}_3\text{-above}$ shows an extent of $d_b = 1.2$ nm, and $\text{CrI}_3\text{-Cl}_3\text{-below}$ and $\text{CrI}_3\text{-Cl}_1$ (d_c and d_d , respectively) show an extent of 1.0 nm. The effects of the larger spatial extent of the distortion mean that there are additional chromium centers that no longer have the full octahedral symmetry surrounding them, thus giving rise to DM terms potentially leading to noncollinear spin solutions with no applied field. It is of particular interest

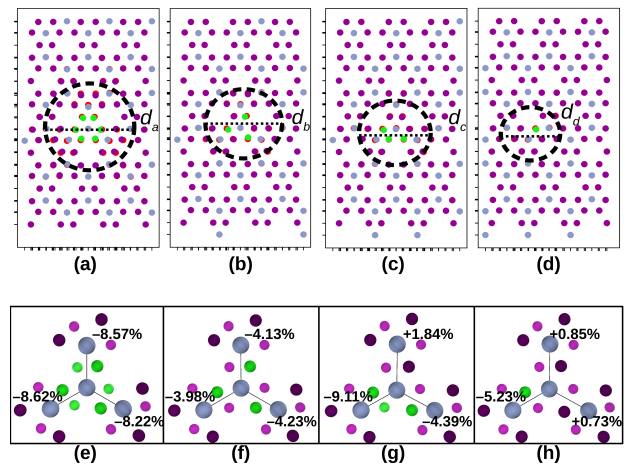


FIG. 2. The optimized geometries of the Cl substituted CrI_3 systems. The initial position of the relevant atoms can be visualized by the red circles. The final geometries are shown with the gray circles representing Cr atoms, the purple circles representing iodine, and the green circles representing chlorine after optimization. The geometries consist of $\text{CrI}_3\text{-Cl}_6$ (a), $\text{CrI}_3\text{-Cl}_3\text{-above}$ (b), $\text{CrI}_3\text{-Cl}_3\text{-below}$ (c), and $\text{CrI}_3\text{-Cl}_1$ (d). e-h show the four central Cr atoms and bound halogen atoms. The text shows the difference in the bond length between the central Cr atom and those neighboring from the pure CrI_3 system and the optimized, doped systems (shown as a $\pm\%$ of the original Cr-Cr bond length).

that both the $\text{CrI}_3\text{-Cl}_6$ and $\text{CrI}_3\text{-Cl}_3\text{-above}$ systems have a symmetric distortion around the central Cr and thus the final geometries are similar, while the $\text{CrI}_3\text{-Cl}_3\text{-below}$ and $\text{CrI}_3\text{-Cl}_1$ systems are less symmetric about the central Cr. In the case of the $\text{CrI}_3\text{-Cl}_3\text{-below}$ and $\text{CrI}_3\text{-Cl}_1$ systems the central Cr is pulled slightly towards the Cr centers that are mediated by Cl atoms leading to a significant distortion to the angles and bond lengths of the surrounding systems.

As a result of the geometric distortions, the inversion symmetry for the doped systems (except the $\text{CrI}_3\text{-Cl}_6$ system) is broken. Thus the DM terms become non-zero. The DM vectors for the Cr atoms within the distorted areas marked in Fig. 2 are plotted in Fig. 3. This effect is localized to the areas with geometric distortion. This can be seen in Fig. 3(d), where the spatial extent of the geometry distortion is significantly less than in the other systems, by the fact that the Cr atoms on the far right (where there was little to no distortion) do not have applicable DM vectors. As previously mentioned, the $\text{CrI}_3\text{-Cl}_6$ system is able to maintain inversion symmetry around the central atom, and as such the DM contributions along each halide pathway cancel out, which is not the case for the other systems.

B. Formation of Spin Bubble

Magnetic skyrmions are local whirls of the spins that both have a fixed chirality and do a full spin rotation.¹

TABLE I. DM vectors calculated using the four-state method of Refs. 6,18. For the CrI₃-Cl₆ and CrI₃-Cl₃_above, the three-fold symmetry surrounding the Cr center is maintained so only one vector is shown. For the other systems, this symmetry is broken and the DM vectors between the central Cr and the three surrounding Cr centers are shown. Cr centers are identified in Fig. 3.

Pair	\mathbf{D}_{ij-X} (meV)	\mathbf{D}_{ij-Y} (meV)	\mathbf{D}_{ij-Z} (meV)	$ \mathbf{D}_{ij} $ (meV)	$ \mathbf{D}_{ij} /J_{ij}$ (meV)
CrI ₃ -Cl ₆ Cr ₁ Cr ₂	-0.28	0.34	-0.22	0.49	7.24
CrI ₃ -Cl ₃ _above Cr ₁ Cr ₂	-1.23	-0.79	-1.48	2.08	2.42
CrI ₃ -Cl ₃ _below Cr ₁ Cr ₂	0.22	0.72	1.02	1.27	0.92
CrI ₃ -Cl ₃ _below Cr ₁ Cr ₃	0.22	0.81	0.21	0.87	0.49
CrI ₃ -Cl ₃ _below Cr ₁ Cr ₄	0.26	-0.02	-0.77	0.81	13.55
CrI ₃ -Cl ₁ Cr ₁ Cr ₂	-0.38	-0.16	1.15	1.22	2.91
CrI ₃ -Cl ₁ Cr ₁ Cr ₃	0.22	0.40	-0.56	0.72	2.77
CrI ₃ -Cl ₁ Cr ₁ Cr ₄	-0.19	-0.53	0.08	0.13	0.49

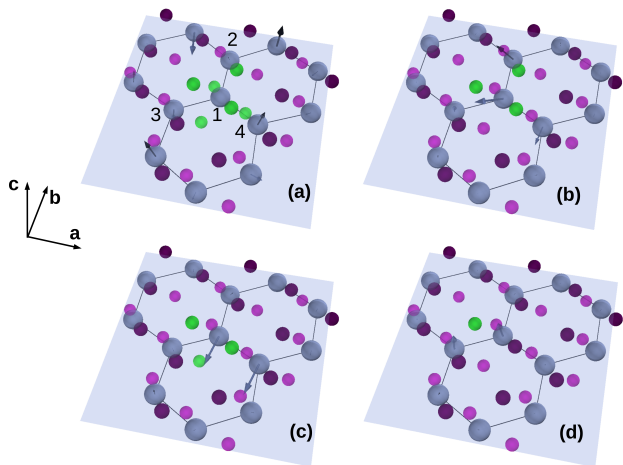


FIG. 3. The DM vectors (in black, determined as by in Ref. 26) on each Cr atom from the geometry optimized, Cl doped systems shown in Fig. 2, CrI₃-Cl₆ (a), CrI₃-Cl₃_above (b), CrI₃-Cl₃_below (c), and CrI₃-Cl₁ (d). Since the DM vectors are only non-zero where the inversion symmetry is broken, and the symmetry breaking is a localized effect, only the atoms that lie roughly within the black circle in Fig. 2 have been plotted. The labeled atoms in (a) are the Cr atoms used in the four-state method to calculate the DM vectors that are reported in Tab. I.

Unfortunately none of the geometries attempted in this study are able to realize a full symmetric skyrmion at zero field. Instead, spin bubbles can be observed in the CrI₃ monolayers arising from spin noncollinear solutions. In the case of the CrI₃-Cl₁ system a spin bubble solution was stabilized as can be seen in Fig. 4. Plotted in Fig. 4 are the atomic clusters shown in Fig. 3 with the magnetization vectors for each Cr atom plotted. It can be noted that in the case of the CrI₃-Cl₃ systems, the spin bubble is unable to manifest and the ferromagnetic solution persists.

In the case of the CrI₃-Cl₁ system, the stabilization by the formation of the spin bubble over the ferromagnetic solution is 25.7 meV/Cr. This energetic difference is larger than what has been previously observed as the stabilization energy from the formation of skyrmions through the use of external fields (~ 3

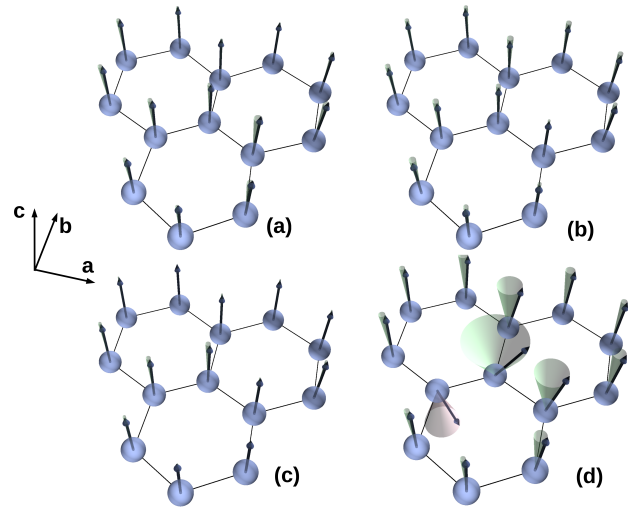


FIG. 4. The canted spin states for each of the systems resulting from the presence of the doped Cl shown by black vectors. The difference between the canted spins and the collinear spins perpendicular to the crystal plane are shown by the cones (where green cones are spins above the layer and red cones are spins beneath the layer).

meV/Cr) is much larger than the cost of a spin rotation (< 1 meV/Cr).² Thus similar to the skyrmions formed through the application of external fields, the spin bubbles are topologically-protected spin configurations. It is interesting to note that while able to form in the CrI₃-Cl₁ system, a spin bubble configuration is not manifested in the CrI₃-Cl₃_below system. Even though, in the CrI₃-Cl₃_below system, there is both a lack of symmetry in the geometry (as in either the CrI₃-Cl₆ or CrI₃-Cl₃_above cases), and there exists a pathway with only a single Cl atom that has a similar geometric distortion to the CrI₃-Cl₁ system. This can be seen in Fig. 2 g and h, with a 4.39% reduction in Cr-Cr distance for the CrI₃-Cl₃_below compared to a 5.23% reduction for the CrI₃-Cl₁. It was previously noted that a minimum field was required in order to induce skyrmions which introduced a distortion between the Cr and I layers in the monolayer CrI₃.² Measuring geometric changes for the systems finds that the CrI₃-Cl₃_below system has a dis-

tortion of 2.2% while the CrI₃-Cl₁ system has a distortion of 3.1%. Given that the distortion of the CrI₃-Cl₃_below system is less than the previously determined minimum may contribute to why a magnetic bubble state is unable to manifest even though there are DM vectors present.

In order to gain insights into the formation of the spin bubble in the CrI₃-Cl₁ system, the DMI vectors were calculated for the Cr atoms shown in Fig. 3. The numerical values for the DM vectors have been tabulated in Tab. I and calculated through the four-state method detailed in Refs. 6,18. For the CrI₃-Cl₆ and CrI₃-Cl₃_above systems only the Cr₁ and Cr₂ pair were calculated due to the presence of the rotational symmetry. For the other systems, the DMI vectors for the nearest neighbors to the central Cr were all explicitly calculated. Previous work has identified that skyrmions are more likely to form when values of D_{ij}/J_{ij} (where $D_{12} = |\mathbf{D}_{ij}|$) are between 0.1-0.2 meV.^{6,27} Larger values of the D_{ij}/J_{ij} value favors faster spin rotations about \mathbf{D}_{ij} leading to smaller skyrmions.²⁷ Our values for D_{ij}/J_{ij} are significantly larger than those reported for previous CrI₃ systems. This is most likely due to the increased localized distortion surrounding the Cr centers. The values for $|\mathbf{D}_{ij}|$ are also larger than those previously reported,⁶ though it should be noted that large values for the DMI vectors have been shown in previous studies and will often introduce other spin configurations than skyrmions.²⁷ Although the CrI₃-Cl₁ (Cr₁,Cr₃) and CrI₃-Cl₃_below (Cr₁,Cr₄) systems are close in geometry and as such expected to both exhibit spin canted solutions, the CrI₃-Cl₃_below system has a $D_{1,4}/J$ value (tabulated in Tab. I) that is too large to manifest a stable spin whirl solution at zero field. In contrast, while the value for D_{ij}/J is larger than in other reports of skyrmion-forming monolayer chromium iodide systems, a spin canted solution is still able to manifest for the CrI₃-Cl₁ system. Since selective doping was able to introduce a spin-canted solution additional studies on alternate geometries and the field effects can be carried out.

IV. CONCLUSION

We show that upon substituting selected Iodine atoms in a CrI₃ monolayer with Cl atoms, localized spin-bubble states form. These spin states arise from the lattice distortions induced by the ionic radii mismatch between the host and the defect species. While distortions are driven by the difference in the X-Cr bond lengths, the interactions between these distortions can induced long-range directional lattice polarization that may enable coupling between spatially-separated spin-bubble states. It was noted that, when these spin-bubble systems formed, they were topologically protected as they were significantly more stable than either the cost of a spin-flip or the stabilization noted by electric-field induced skyrmions. This work provided an important step toward manifesting skyrmions at conditions that would be useful for spin-

tronic applications by potentially reducing the field required and increasing the operating temperature through controlled doping of CrI₃ monolayers.

V. ACKNOWLEDGEMENT

The work was supported by the Northwest Institute for Materials Physics, Chemistry, and Technology (NW IMPACT), and the University of Washington Molecular Engineering Materials Center (DMR-1719797). This work was facilitated through the use of advanced computational, storage, and networking infrastructure provided by the Hyak supercomputer system and funded by the STF at the University of Washington.

-
- * xsli@uw.edu
- ¹ A. Fert, N. Reyren, and V. Cros, *Nat. Rev.* **2**, 17031 (2017).
- ² J. Liu, M. Shi, P. Mo, and J. Lu, *AIP Advances* **8**, 055316 (2018).
- ³ T. Moriya, *Phys. Rev.* **120**, 91 (1960).
- ⁴ J. L. Lado and J. Fernández-Rossier, *2D Mater.* **4**, 035002 (2017).
- ⁵ J. Liu, M. Shi, J. Lu, and M. P. Anantram, *Phys. Rev. B* **97**, 054416 (2018).
- ⁶ C. Xu, J. Feng, S. Prokhorenko, Y. Nahas, H. Xiang, and L. Bellaiche, *Phys. Rev. B*, 060404 (2020).
- ⁷ A. K. Behera, S. Chowdhury, and S. R. Das, *Appl. Phys. Lett.*, 232402 (2019).
- ⁸ B. Huang, G. Clark, E. Navarro-Moratalla, D. R. Klien, R. Cheng, K. L. Seyler, D. Zhong, E. Schmidgall, M. A. McGuire, D. H. Cobden, W. Yao, D. Xiao, P. Jarillo-Herrero, and X. Xu, *Nature* **546**, 270 (2017).
- ⁹ B. Huang, genevieve Clark, D. R. Klein, D. MacNeil, E. Navarro-Moratalla, K. L. Seyler, N. Wilson, M. A. McGuire, D. H. Cobden, D. Xiao, W. yao, P. Jarillo-Herrero, and X. Xu, *Nat. Nanotechnol.* **13**, 544 (2018).
- ¹⁰ T. Song, Z. Fei, M. Yankowitz, Z. Lin, Q. Jiang, K. Hwangbo, Q. Zhang, B. Sun, T. Taniguchi, K. Watanabe, M. A. McGuire, D. Graf, T. Cao, J.-H. Chu, D. H. Cobden, C. R. Dean, D. Xiao, and X. Xu, *Nat. Mater.*, 1476 (2019).
- ¹¹ N. Sivadas, S. Okamoto, X. Xu, C. J. Fennie, and D. Xiao, *Nano Lett.* **18**, 7658 (2018).
- ¹² M. A. McGuire, hemant Dixit, V. R. Cooper, and B. C. Sales, *Comp. Mater.* **27**, 612 (2015).
- ¹³ C. Felser, G. H. Fecher, and B. Balke, *Angew. Chem.* **46**, 688 (2007).
- ¹⁴ B. Behin-Aein, J.-P. Wang, and R. Wiesendanger, *MRS Bull.* **39**, 696 (2014).
- ¹⁵ L. L. Handy and N. W. Gregory, *J. Am. Chem. Soc.*, 5049 (1950).
- ¹⁶ C. Lee, H. Y. Kwon, N. J. Kim, H. G. Yoon, C. Song, D. B. Lee, J. W. Choi, Y.-W. Son, and C. Won, *J. Magn. Magn. Mater.* **501**, 166447 (2020).
- ¹⁷ N. D. Mermin and H. Wagner, *Phys. Rev. Lett.* **17**, 1133 (1966).
- ¹⁸ C. Xu, J. Feng, H. Xiang, and L. Bellaiche, *Comp. Mater.*, 57 (2018).
- ¹⁹ M. A. McGuire, *Crystals* **7**, 121 (2017).
- ²⁰ P. W. Anderson, *Phys. Rev.* **79**, 350 (1950).
- ²¹ G. Kresse and J. Furthmüller, *Comput. Mater. Sci.* **6**, 15 (1996).
- ²² G. Kresse and J. Furthmüller, *Phys. Rev. B* **54**, 11169 (1996).
- ²³ P. E. Blöchl, *Phys. Rev. B* **50**, 17953 (1994).
- ²⁴ J. P. Perdew, K. Burke, and M. Ernzerhof, *Phys. Rev. Lett.* **77**, 3865 (1996).
- ²⁵ S. Grimme, J. Antony, S. Ehrlich, and S. Krieg, *J. Chem. Phys.* **132**, 154104 (2010).
- ²⁶ F. Keffer, *Phys. Rev.* **126**, 896 (1961).
- ²⁷ A. Fert, V. Cros, and J. Sampaio, *Nat. Nano.* **8**, 152 (2013).